




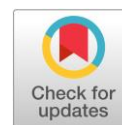


# Towards controlling the morphology of cobalt loaded nanocomposites in polyol process with polyethylene glycol

Anastasia Burmatova, Artur Khannanov \* , Liana Zubaidullina, Dmitry Emelianov , Olga Mostovaya, Ivan Stoikov , Nikolay Ulakhovich , Marianna Kutyreva \* 

A.M. Butlerov Chemical Institute, Kazan Federal University, Kazan 420008, Russia

\* Corresponding authors: [arthann@gmail.com](mailto:arthann@gmail.com); [mkutyreva@mail.ru](mailto:mkutyreva@mail.ru)



This paper belongs to a Regular Issue.

## Abstract

The polyol process is one of the simple, efficient and productive methods for the synthesis of metal loaded polymer composites. Functional properties of metal-polymer nanocomposites are determined by chemical composition, size and morphology of their particles. Finding effective ways to control the nanoparticle's properties during the polyol process is a crucial task. The effect of molar ratio  $M^{n+}/OH_{PEG}$  on the formation of cobalt loaded metal-polymer nanocomposites during a one-pot two-component polyol process by polyethylene glycol with  $M_r = 4000 \text{ g}\cdot\text{mol}^{-1}$  (PEG) was studied. The PEG-based polyol process and the formation of cobalt nanophase were studied at molar ratios  $v_{Co^{2+}}/v_{OH(PEG)} = 1:1, 1:10, 1:100$  and  $1:500$  using UV-Vis, diffuse reflectance IR and ATR FT-IR spectroscopy, nanoparticle tracking analysis (NTA), dynamic light scattering (DLS). It was found that PEG can act as a reducing agent and stabilizing matrix for the cobalt nanophase at a ratio higher than  $M^{n+}/OH_{PEG} = 1:10$ . The composition and morphology of Co/PEG nanocomposites were determined by XRD and TEM methods. Two types of spheroid particles with average diameters of  $88 \pm 55 \text{ nm} / 8 \pm 4 \text{ nm}$  and  $12 \pm 3 \text{ nm} / 3 \pm 1 \text{ nm}$ , respectively, represent Co/PEG nanocomposites  $1:500$  and  $1:100$ . Scaly structures with a diameter of  $15 \pm 5 \text{ nm}$  are formed at a molar ratio of  $v_{Co^{2+}}/v_{OH(PEG)} = 1:10$ . An increase in the  $Co^{2+}$  content in the PEG-based polyol process leads to the immobilized cobalt nanophase  $Co_3O_4$  ( $1:500$ ),  $Co^0/CoO$  ( $1:100$ ),  $CoO$  ( $1:10$ ) in PEG. Co/PEG nanocomposites are hemocompatible. The  $HC_{50}$  value depends on the composition and morphology of the nanoparticles.

## Keywords

polyol process  
polyethylene glycol  
cobalt  
nanocomposites  
biocompatibility

## Key findings

- The effect of  $M^{n+}/OH_{PEG}$  molar ratio on the formation of cobalt loaded metal-polymer nanocomposites during a one-pot two-component polyol process by polyethylene glycol with  $M_r = 4000 \text{ g}\cdot\text{mol}^{-1}$  (PEG) was studied.
- Controlling the size and structure of Co/PEG composite particles allows maintaining their biocompatibility.
- Composites Co/PEG containing only cobalt oxides ( $CoO$  or  $Co_3O_4$ ) and having dimensions above  $5 \text{ nm}$  are hemocompatible. The hemolytic activity of  $HC_{50}$  can reach  $6.12 \text{ g}\cdot\text{ml}^{-1}$ .

© 2023, the Authors. This article is published in open access under the terms and conditions of the Creative Commons Attribution (CC BY) license (<http://creativecommons.org/licenses/by/4.0/>).



## 1. Introduction

Nanometallic polymer composite and hybrid materials have unique properties and wide application possibilities in various fields of science and technology, including catalysis, electronics and biomedicine [1–5]. The size, composition, structure and morphology (shape and spatial organization)

of metal nanophase all play key roles in tuning the functional activity and target properties of the metal-polymer nanocomposite. In turn, the characteristics of material particles in general and metal nanophase particles in particular are determined by the components of the medium and the synthesis conditions. In this case, the simplest version of the reaction system for the production of metal-polymer

nanomaterial is a two-component system consisting only of a metal precursor compound and polymer nanoparticles.

Among the existing synthesis methods that make it possible to obtain metal nanoparticles in a medium with a limited composition the polyol process is the most promising. Polyol synthesis is a widely used method for preparing metal-loaded composite nanomaterials due to its numerous advantages such as simplicity, versatility, and control of the size and morphology of metal nanoparticles [6–8]. The metal precursor and the polyol, which is both a reducing agent and a stabilizer of metal nanoparticles, are the main reagents in this method.

The choice of polyol and synthesis conditions plays a decisive role in determining the composition, structure, size and morphological characteristics of the resulting nanocomposite particles. Traditionally, this synthesis method uses linear low-molecular-weight alcohols: ethylene glycol [9, 10], propylene glycol [11], etc. In addition, in the polyol process, linear polymeric polyols can be used, e.g., polyvinyl alcohol [12], hyperbranched polyester polyols [13], etc.

Water-soluble polymeric polyols are the most promising in the synthesis of metal loaded polymer nanocomposites which have great potential in biomedicine and ecology. In addition, the ability of polymeric polyols with high molecular weight to control the size and morphology of the metal nanophase is superior to that of low-molecular-weight stabilizers. However, most water-soluble polyols, such as polyvinyl alcohol [14], poly(N-vinylpyrrolidone) [10, 15], polylactic acid [16], PEG [17] are used only as stabilizers in the polyol process. The function of a reducing agent in this case is performed by a low-molecular-weight polyhydric alcohol.

Among the designated polymeric polyols polyethylene glycol (PEG) has the greatest potential for implementing the polyol process in a two-component reaction system [18–23]. PEG has a number of desirable characteristics including high thermal stability, nontoxicity, excellent solvation ability, and the ability to reduce metal precursors under suitable reaction conditions [24,25]. In addition, the advantage of PEG is its commercial availability in different molecular weights, which allows controlling the morphology and functional activity of materials.

Using the two-component polyol process with PEG, nanoparticles of some metals were obtained, and areas of their promising application were identified. For example, nanoparticles of gold [18] and silver [19, 20] synthesized by the PEG-based polyol process with PEG 200–20000 demonstrate antimicrobial activity and potential in electronics and surface-enhanced Raman spectroscopy. It was demonstrated that the size of the silver nanoparticles decreases with decreasing molecular weight of PEG [20]. It was shown that varying the molecular weight and concentration of PEG in the synthesis makes it possible to synthesize iron nanoparticles of cubic and polyhedral shape for PEG-200 [21], spherical shape for PEG-300 [22] as well as spherical bimetallic nanoparticles of cobalt and iron [23] with specified sizes and morphology. Prospects for the applications of

synthesized iron nanoparticles are in areas such as magnetic resonance imaging (MRI), drug delivery, and magnetic separation methods.

Thus, polyethylene glycol of various grades can act as a bifunctional agent (a reducing agent and a stabilizer at the same time) in the synthesis of nanoparticles of various metals. According to most authors, the molecular weight of PEG determines the size, composition and morphology of metal nanoparticles obtained by PEG-based polyol process [18]. However, one of the leading factors influencing the morphology of the metal nanophase in the polyol process is the  $M^{n+}/OH_{polyol}$  ratio. It was found that for low-molecular-weight ethylene glycol [26] and polyvinyl alcohol [14] the load of the metal phase and particle sizes decrease linearly with a decrease in the mole fraction of alcohol in situ. Establishing the patterns of the influence of the  $M^{n+}/OH$  molar ratio in the PEG-based polyol process will allow determining new approaches to controlling the composition, size and morphology of the metal loaded nanocomposites.

The goal of this work was to propose an approach to controlling the size, composition and morphology of cobalt loaded nanocomposite particles during the PEG-based polyol process, as well as to evaluate the properties and functional activity of the cobalt-containing nanocomposites.

## 2. Materials and Methods

### 2.1. Materials

For the synthesis of cobalt-containing nanocomposites (Co/PEG), polyethylene glycol 4000 – PEG 4000 (Sigma-Aldrich, CAS: 25322-68-3, average  $M_r = 4000 \text{ g}\cdot\text{mol}^{-1}$ , hydroxyl number  $28 \text{ mg KOH}\cdot\text{g}^{-1}$ ) and  $\text{CoCl}_2\cdot 6\text{H}_2\text{O}$  (99%, Alfa Aesar) as a cobalt precursor were used. To study the hemolytic activity of Co/PEG, blood from healthy donors was obtained from the blood donor center in Kazan. The blood was anticoagulated with 3% sodium citrate. Co/PEG samples for TEM were prepared in methanol. To study the properties of Co/PEG we used deionized water ( $\Omega = 18.2 \text{ M}\Omega\cdot\text{cm}$  at  $25 \text{ }^\circ\text{C}$ ,  $\chi = 0.055 \text{ }\mu\text{S}/\text{cm}$ , particle number of  $0.22 \text{ }\mu\text{m}/\text{ml} < 1$ ) and phosphate buffered saline (PBS) with  $\text{pH} = 3.58$ .

### 2.2. Equipment

The FT-IR spectra were recorded on a Spectrum 400 (PerkinElmer, Connecticut, USA) ATR spectrometer. The FT-IR spectra from  $4000$  to  $400 \text{ cm}^{-1}$  were considered in this analysis. The spectra were measured with  $1 \text{ cm}^{-1}$  resolution and 64 scan averaging.

To establish the mechanism of oxidation of PEG, FT-IR spectra were recorded on a Spectrum 400 Fourier spectrometer (PerkinElmer, Connecticut, USA) with a diffuse reflectance accessory with a compact temperature controller "PIKE technologies" in the temperature range  $35$ – $210 \text{ }^\circ\text{C}$ ,  $4000$ – $400 \text{ cm}^{-1}$  ( $1 \text{ cm}^{-1}$  resolution, 16-scan accumulation, shooting range  $4000$ – $400 \text{ cm}^{-1}$ ).

The electronic absorption (UV-Vis) spectra were recorded on a Lambda 750 (PerkinElmer, Connecticut, USA)

spectrometer in the wavelength range of 200–1000 nm at  $T = 25 \pm 0.01$  °C, using a temperature-maintaining system including a cell holder, circulating thermostat Julabo MB-5A, and a Peltier PTP-1 thermostat. Quartz cells with a thickness of 1 cm were used for the measurements. The measurement accuracy for absorbance ( $A$ ) was  $\pm 1\%$ .

The colloidal properties were studied by the Nanoparticle Tracking Analysis (NTA) method on a NanoSight LM – 10 instrument (Malvern Panalytical, Malvern, England). CMOS cameras C11440-50B with an FL-280 Hamamatsu Photonics (Shizuoka, Japan) image capture sensor used as a detector. The measurements were taken in a special cuvette for aqueous solutions, equipped with a 405 nm laser (version CD, S/N 2990491) and a sealing ring made of Kalrez material. The temperature was taken with an OMEGA HH804 contact thermometer (Engineering, Inc., Stamford, CT, USA) for all measurements. The samples for analysis were injected into the measuring cell with a 1 mL glass 2-piece syringe (tuberculin) through the luer-lock fitting (Hamilton Company, Reno, NV, USA). To increase the statistical dose, the sample was pumped through the measuring chamber using a piezoelectric dispenser. Each sample was detected sequentially 6 times; the total recording time was 60 s. For processing the footage from the Nanosight instrument, NTA 2.3 (build 0033) and OriginPro software were used; the Gauss function was employed as described previously [27, 28]. The detailed procedures are described elsewhere [29, 30]. The hydrodynamic size ( $D_h$ ) was calculated with the two-dimensional Einstein–Stokes equation [31].

Thermogravimetric analysis (TG) were performed using a thermal analyzer STA 449 F1 Jupiter (Netzsch GmbH, Selb, Germany) with the temperature rate of  $10 \text{ K} \cdot \text{min}^{-1}$  in an argon atmosphere with the total flow rate of  $75 \text{ mL} \cdot \text{min}^{-1}$ . The analysis was performed in a temperature range of 40–600 °C in an Al crucible with a volume of 40  $\mu\text{L}$  with lids having 3 holes, each 0.5 mm in diameter.

Experiments on the thermal stability of the composites were performed on a precision thermobalance TG209 F1 Libra (Netzsch GmbH, Selb, Germany) in synthetic air atmosphere.

Powder diffraction patterns (XRD) of composites were taken on a MiniFlex 600 diffractometer (Rigaku, Japan) equipped with a D/tex Ultra detector. Cu  $K\alpha$  radiation (40 kV, 15 mA) was used in the  $2\theta$  angle range from  $3^\circ$  to  $60^\circ$  in  $0.02^\circ$  steps with a dwell at each point of 0.24 s without rotation.

The transmission electron microscope (TEM) imaging was carried out in the Hitachi HT7700 (Tokyo, Japan) Excellence microscope at an accelerating voltage of 100 kV in the TEM mode. The size and shape of the synthesized nanoparticles were estimated using ImageJ software.

Ultrasonic treatment of dispersions for sorption studies was carried out in a Sapphire ultrasonic bath ( $T = 25$  °C, operating frequency 35 kHz).

### 2.3. Synthesis of polymer-stabilized cobalt nanoparticles Co/PEG by polyol process

Polyethylene glycol PEG (3 g) and  $\text{CoCl}_2 \cdot 6\text{H}_2\text{O}$  (0.0007 g, 0.0036 g, 0.0356 g and 0.3562 g) was heated under constant stirring at 70 °C until a homogeneous mixture were formed. Molar ratios  $M^{n+}/\text{OH}_{\text{polyol}}$  were  $V_{\text{Co(II)}}/V_{\text{OH(PEG)}} = 1:500$  for Co/PEG-1, 1:100 for Co/PEG-2, 1:10 for Co/PEG-3 and 1:1 for Co/PEG-4. The resulting mixture was left for 24 h at room temperature and then heated to 160 °C in 10 °C increments under constant stirring. Solid NaOH was added to all samples (molar ratio of  $V_{\text{NaOH}}/V_{\text{Co(II)}} = 1:10$ ) before the heating stage. The formation of cobalt loaded nanocomposites Co/PEG was accompanied by a color change from blue to brown for Co/PEG-1 and Co/PEG-2 and from blue to green for Co/PEG-3 and Co/PEG-4.

### 2.4. Sorption studies

The sorption of  $\text{Co}^{2+}$  ions by polyol PEG matrix was carried out in static conditions in  $\text{H}_2\text{O}$ . A series of solutions were prepared with a constant concentration of PEG ( $0.125 \text{ g} \cdot \text{mL}^{-1}$ ) and a variable concentration of salt  $\text{CoCl}_2 \cdot 6\text{H}_2\text{O}$  ( $0.05$ – $0.8 \text{ mol} \cdot \text{L}^{-1}$ ) in  $\text{H}_2\text{O}$ . The mixtures were treated with ultrasound for 1 h and incubated at room temperature for 24 h. The resulting associate  $[\text{Co}^{2+} - \text{PEG}]$  was separated by centrifugation ( $v = 10,000 \text{ rpm}$ ,  $t = 5 \text{ min}$ ) and the free concentration of the  $\text{Co}^{2+}$  ion in the solution was determined by the UV–Vis spectrophotometry according to the calibration function at  $\lambda = 511 \text{ nm}$ :

$$A_{530} = (6.3136 \pm 0.022) \cdot c_{\text{Co(II)}} - (0.0775 \pm 0.001) \quad (1)$$

$$R = 0.9989$$

Intrinsic absorption of PEG in solution was taken into account in the baseline. The absorption of  $\text{CoCl}_2 \cdot 6\text{H}_2\text{O}$  solutions at the same concentrations without the PEG polymer was taken into account in the control experiment. The sorption isotherm was plotted in the coordinates  $c^{\text{S}}_{\text{Co}^{2+}}$  vs  $c^{\text{O}}_{\text{Co}^{2+}}$  where  $c^{\text{S}}_{\text{Co}^{2+}}$  is the sorbed concentration of  $\text{Co}^{2+}$  and  $c^{\text{O}}_{\text{Co}^{2+}}$  is the initial concentration of  $\text{Co}^{2+}$  in the solution.

### 2.5. Study of biocompatibility

Biocompatibility was assessed based on the hemolysis coefficient (HC, %) [32]. Blood erythrocytes from healthy donor were separated by centrifugation ( $5000 \times g$ , 5 min) at 4 °C, washed three times with phosphate-buffered saline (PBS) and used immediately after isolation. The red blood cells (RBC) were suspended in Co/PEG nanocomposite dispersions in PBS to study hemolysis at a hematocrit of 1% and incubated for 0.5 h at a temperature of 20 °C. The incubated suspensions were centrifuged at  $1000 \times g$  for 5 min. For reference the RBC were treated with double-distilled water which caused 100% hemolysis. The HC (%) was determined from the released hemoglobin in the supernatants and measured spectrophotometrically by absorbance at 540 nm:

$$\text{HC} [\%] = \frac{A - A_-}{A_+ - A_-} \cdot 100\%, \quad (2)$$

where  $A$  is the optical density of the RBC incubated with nanocomposites,  $A_-$  is the optical density of the sample in PBS, and  $A_+$  is the optical density of the RBC in water (100% hemolysis). The nanocomposites themselves contributed no more than 0.1% of the absorbance at 540 nm. The results are expressed as mean  $\pm$  standard deviation,  $n = 5$ . The minimum effective concentration of the Co/PEG nanocomposite that caused hemolysis in 50% of red blood cells ( $HC_{50}$ ) was determined.

### 3. Results and Discussion

The effect of  $M^{n+}/OH_{polyol}$  molar ratio on the formation of cobalt loaded metal-polymer nanocomposites during a one-pot two-component polyol process with polyethylene glycol (PEG) was studied. Polyethylene glycol with a molecular weight of 4000 Da (PEG 4000) was used as a reducing/stabilizing agent and a medium in the synthesis. The choice of PEG 4000 (hereinafter referred to as PEG) is due to its water solubility, reducing activity, stabilizing properties and high biocompatibility, which makes it possible to further use the nanocomposites in biomedicine [33].

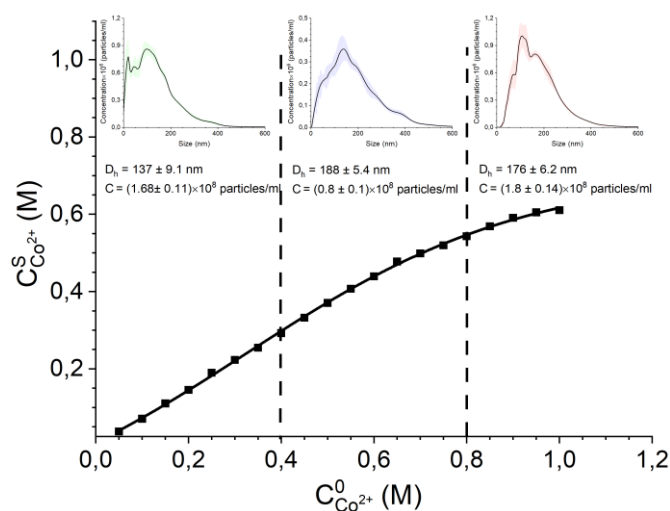
#### 3.1. Study of the interaction of $Co^{2+}$ ions with PEG

The formation of  $[Co^{2+}-PEG]$  associates is the starting stage of the PEG based polyol process. The interaction of  $Co^{2+}$  ions with PEG polyol was studied using UV-Vis and NTA methods. According to NTA data PEG in aqueous solution is polydisperse and forms aggregates with an average hydrodynamic diameter  $D_h^{mean} = 149 \pm 9.6$  nm and a concentration of particles  $C = (0.42 \pm 0.02) \cdot 10^8$  particles·ml<sup>-1</sup> (Figure S1A). According to fractional analysis data using Gaussian approximation, four types of PEG aggregates with hydrodynamic diameters of 67, 107, 158, 309 nm were formed in the solution.

The parameters of immobilization of  $Co^{2+}$  ions into polyol aggregates were estimated from sorption data. The study of the electronic absorption spectra of  $CoCl_2$ -PEG dispersions at a constant polyol concentration and various concentrations of inorganic salt showed that the immobilization of cobalt ions is accompanied by the formation of localized coordination units  $CoO_n$  with tetrahedral geometry (Figure S2). This is confirmed by the presence of a d-d transition band at 511 nm, followed by a shoulder at 476 nm. It can be assumed that the oxygen atom of hydroxyl groups of PEG participates in coordination with  $Co^{2+}$  ions [34]. The sorption isotherm of  $Co^{2+}$  ions on PEG in  $H_2O$  and NTA analysis data are presented in Figure 1.

The Langmuir isotherm model was used to find the  $A_\infty$  and  $K_L$  values from the  $1/C^S - 1/C^0$  dependence plot (Figure S3).

According to the calculations, the sorption constant was  $K = 1.979$  ml·mM<sup>-1</sup>, and the value of the limiting sorption of  $Co^{2+}$  was  $A_\infty = 4.572$  mM·g<sup>-1</sup>. According to the sorption data the preorganization of  $Co^{2+}$  ions in the PEG matrix occurs with the formation of ion-polymer associates. The molar ratio  $V_{Co^{2+}}/V_{OH\ polyol}$  during preorganization was 1:9.



**Figure 1** Sorption isotherm of  $Co^{2+}$  ions by PEG in  $H_2O$  solution and data of NTA measurements in  $CoCl_2$ -PEG aqueous solution ( $C_{PEG} = 0.125$  g·ml<sup>-1</sup>,  $C_{Co^{2+}} = 0.05$ -1 M).

NTA control of the  $[Co^{2+}-PEG]$  system showed that the process of immobilization of cobalt ions is accompanied by a pronounced decrease in the polydispersity of the system and an increase in both the average hydrodynamic diameter to  $D_h = 176 \pm 6.2$  nm and the particle concentration to  $C = (1.8 \pm 0.14) \cdot 10^8$  particles·ml<sup>-1</sup>. Fractional analysis of the evolution of the concentration profile with a Gaussian fit (Figure S1b, c, d) shows that the system consists of ion-polymer aggregates with hydrodynamic diameters of 71, 110 and 163 nm.

#### 3.2. Study of PEG based polyol process for synthesis of Co/PEG nanocomposites

Polyethylene glycol must act as a bifunctional agent (a reducer of cobalt ions and a stabilizer of the resulting clusters and cobalt nanoparticles) when polyol process is carried out in a two-component medium. Therefore, the polyol must be used in excess. To establish the concentration conditions of the PEG-based polyol process in two-component system, cobalt-containing nanocomposites were synthesized at various  $V_{Co^{2+}}/V_{OH(PEG)}$  molar ratios. The synthesis was carried out in a PEG melt at a constant PEG concentration and with a varying the  $CoCl_2$  concentration. The reduction of  $Co^{2+}$  ions immobilized in PEG aggregates was carried out by stepwise heating of the  $CoCl_2$ -PEG reaction mixture to 160 °C. The total heating time was 5 h. The formation of a nanocomposite in Co/PEG in the melt was accompanied by the following color transitions: blue – blue – brown for Co/PEG-1 and Co/PEG-2, blue – blue – green for Co/PEG-3 and Co/PEG-4 (Figure S4-S6). All nanocomposites have exceptional colloidal stability.

UV-Vis spectroscopy was used to obtain the data on formation of cobalt nanophases in the polyol process. To identify the absorption bands the electronic spectra of aqueous dispersions of the synthesized Co/PEG nanocomposites were deconvoluted using the Gaussian functions. All Co/PEG samples are represented by cobalt cluster particles with  $\lambda_{SPR} = 242$ -244 nm [35]. A shoulder in the region of 332-371 nm was observed in the spectra of all samples of



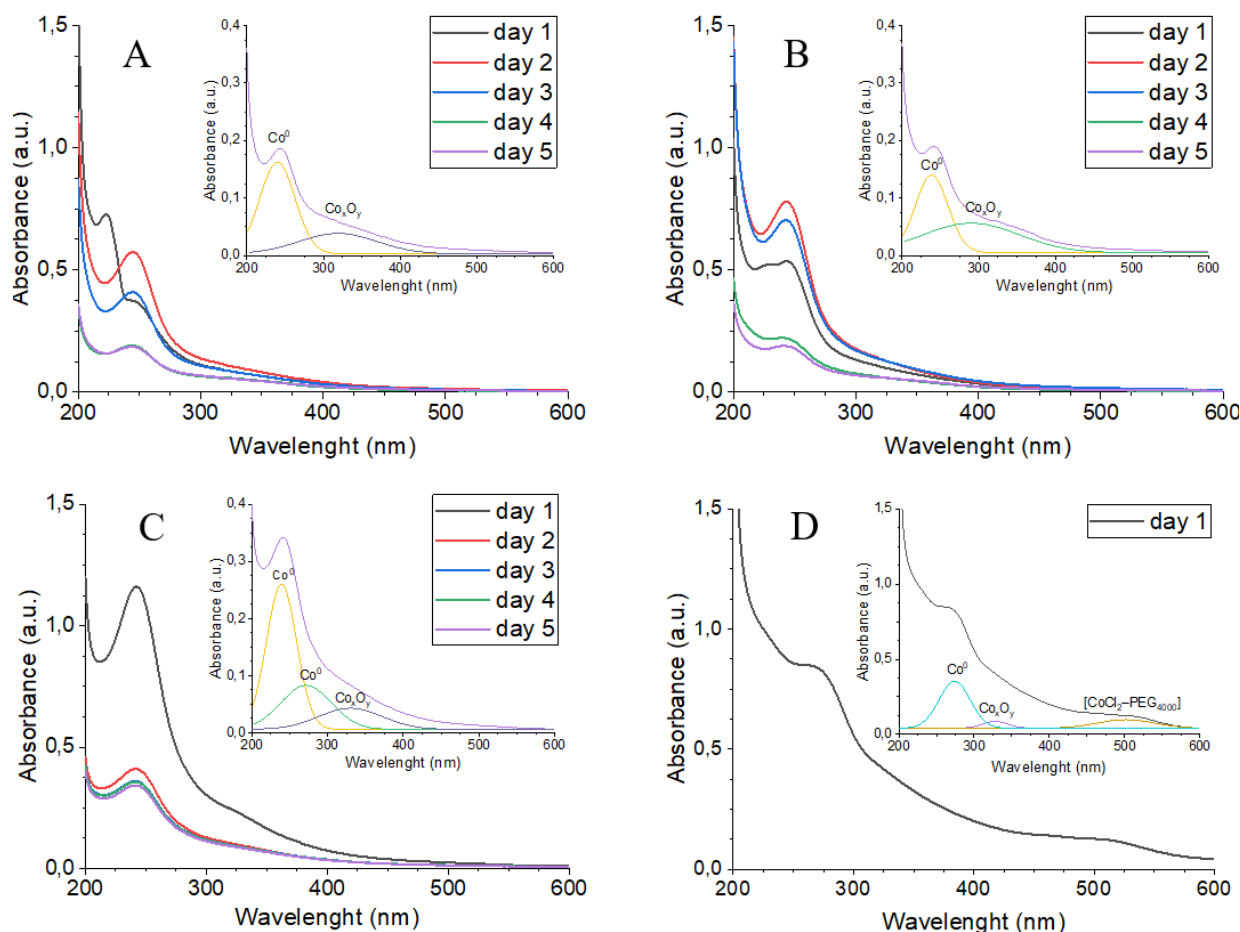
Co/PEG nanocomposites. This indicates the presence of cobalt oxide  $\text{Co}_x\text{O}_y$  [36, 37] in the nanocomposites. Additionally, a weak absorption band at 507 nm is observed in the spectra of Co/PEG-4 due to the presence of complexed  $\text{Co}^{2+}$  ions in the nanocomposite as a result of their incomplete reduction. Thus, the bifunctional (reducing and stabilizing) activity of PEG for the polyol process is limited by the ratio  $V_{\text{Co}^{2+}}/V_{\text{OH(PEG)}} = 1:10$ .

This corresponds to the molar ratio of the functional components of the polyol process during the formation of ion-polymer associates at the preorganization stage. Therefore, the Co/PEG-4 nanocomposite was not studied in further work. Stabilization of the metal nanophase in the Co/PEG-1-3 composites occurred after 5 days due to the Ostwald ripening process (Figure 2).

The particle size distribution of Co/PEG nanocomposites was studied using NTA and DLS analysis data after 1 and 14 days (Table 1, Figure S7). The particles of Co/PEG nano-

composites are characterized by a bimodal distribution according to DLS and a monomodal distribution according to NTA, since for the NTA method the size range  $D_h < 10$  nm lies below the detection threshold. The hydrodynamic diameters of the corresponding particle fractions according to the NTA and DLS methods are close.

To discuss the size characteristics of particles with  $D_h > 10$  nm, the data from the NTA method were used. The dispersion characteristics of the system in this case are better, and the value of  $D_h$  is determined more accurately. It was found that the PEG based polyol process allows obtaining Co/PEG nanocomposites with two types of particles: smaller Co/PEG particles with  $D_{\text{hDLS}} = 3.8 \pm 0.7$  nm, and particles with  $D_{\text{hNTA}} = 130 \pm 2$  nm for Co/PEG-1 and  $D_{\text{hNTA}} = 127 \pm 2.5$  nm for Co/PEG-2. The decrease in the degree of polydispersity of particles in both Co/PEG-1 and Co/PEG-2 and stabilization of  $D_h$  values with a change in the ratio between particle fractions were observed after 14 days.



**Figure 2** Evolution of electronic absorption spectra of dispersions of individual polymer-stabilized Co/PEG-1 (a), Co/PEG-2 (b), Co/PEG-3 (c), Co/PEG-4 (d) nanoparticles in water ( $C_{\text{Co/PEG}} = 0.01 \text{ g}\cdot\text{ml}^{-1}$ ) and interpolation of absorption band from Gauss distribution function ( $R^2 = 99.9$ ,  $\chi^2 = 4.85 \cdot 10^{-5}$ ).

**Table 1** Particle sizes of the nanocomposites Co/PEG ( $C_{\text{Co/PEG}} = 10 \text{ mg}\cdot\text{ml}^{-1}$ ) in  $\text{H}_2\text{O}$ , obtained using NTA and DLS.

Sample	1 day				14 day			
	$D_{\text{h}}^{\text{DLS}}$ , nm	$\text{PDI}^{\text{DLS}}$	$D_{\text{h}}^{\text{NTA}}$ , nm	$C_{\text{Co/PEG}}^{\text{NTA}} \cdot 10^8$ , particles/ml	$D_{\text{h}}^{\text{DLS}}$ , nm	$\text{PDI}^{\text{DLS}}$	$D_{\text{h}}^{\text{NTA}}$ , nm	$C_{\text{Co/PEG}}^{\text{NTA}} \cdot 10^8$ , particles/ml
Co/PEG-1	$3.5 \pm 0.46$ $162 \pm 35$	$0.432 \pm 0.045$	$130 \pm 2$	$8.67 \pm 0.45$	$3.76 \pm 0.66$ $142 \pm 31$	$0.330 \pm 0.103$	$130 \pm 8$	$6.89 \pm 0.80$
Co/PEG-2	$3.86 \pm 0.81$ $137 \pm 20$	$0.467 \pm 0.077$	$127 \pm 2$	$5.72 \pm 0.57$	$3.34 \pm 0.46$ $135 \pm 30$	$0.319 \pm 0.061$	$119 \pm 4$	$11.42 \pm 1.32$

For Co/PEG-1 the fraction of the smaller particles increases (Figure S7 a, b) while the concentration of larger particles decreases. For Co/PEG-2 the opposite effect on smaller particles was observed (Figure S7 c, d) and the concentration of larger particles doubles. In general, increasing the loading of cobalt in Co/PEG-2 leads to a decrease in the hydrodynamic particle diameter  $D_h$ . Co/PEG-3 nanocomposite particles have high polydispersity, which does not allow DLS and NTA experiments to be carried out correctly.

### 3.3. IR - study of PEG oxidation and nanocomposite Co/PEG

Diffuse reflectance IR spectroscopy was used to study the oxidation process of PEG with forming of Co/PEG-3 sample. The process of oxidation of the hydroxide groups of the polyol begins at 160 °C (Figure 3). In this case, the oxidation of the hydroxide groups of polyethylene glycol occurs to carboxyl groups. This is indicated by the appearance of a signal at 1745  $\text{cm}^{-1}$  corresponding to carbonyl groups in the COOH fragment. An increase in the intensity of the signal related to the stretching vibrations of the OH group at 3495  $\text{cm}^{-1}$  also confirms the formation of carbonyl groups. At 160 °C in the region of 1200-1100  $\text{cm}^{-1}$ , a restructuring of the deformation vibrations of the C-O polyol is observed. The appearance of a signal at 1186  $\text{cm}^{-1}$  related to C-O indicates the formation of carboxyl groups.

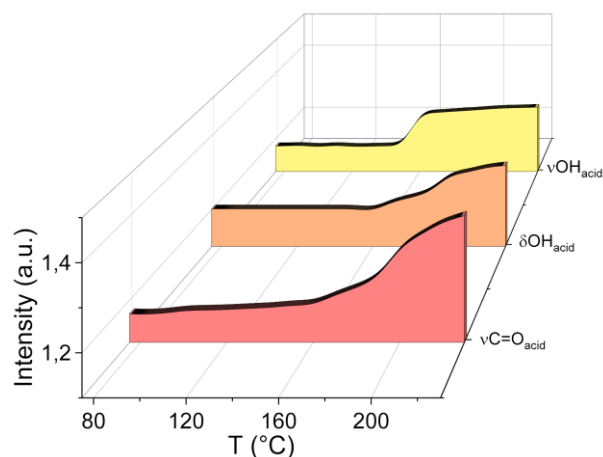
Local centers of stabilization of metallic cobalt nanoparticles in the PEG matrix were established using ATR FT-IR spectroscopy (Figure 4). The FT-IR spectra are characterized by the presence of an absorption band at 668  $\text{cm}^{-1}$  due to the  $\nu_{(\text{Co(II)}-\text{O})}$  stretching vibrations of cobalt oxide on the surface of the metal nanoparticle for all Co/PEG samples. [38]. In the spectra of Co/PEG nanocomposites a decrease in intensity and a shift in the band of stretching vibrations of PEG hydroxyl groups were recorded. Also bands at 1749  $\text{cm}^{-1}$  and 1723  $\text{cm}^{-1}$ , which can be due to stretching vibrations of the free and bound-to-surface-cobalt atoms of the carbonyl group C=O in the resulting acid fragment [39]. IR data suggest that the surface of the metal nanoparticle is stabilized due to electrostatic interactions with the hydroxyl groups of nonoxidized PEG and the carboxyl moieties of the oxidized polyol.

According to UV-Vis and FT-IR data the polyol-process of formation of a cobalt loaded nanocomposite in a PEG medium can be represented in accordance with Figure 5.

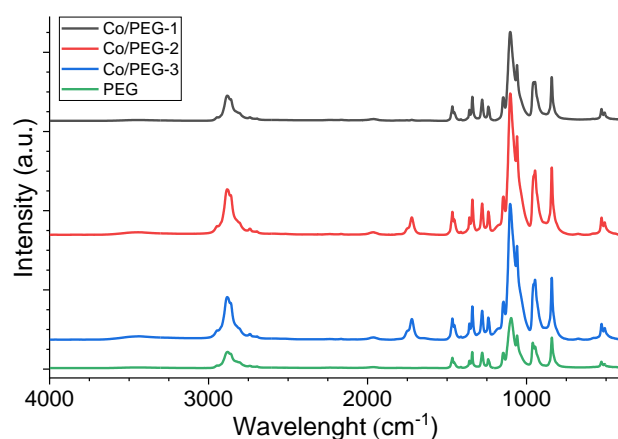
### 3.4. Morphology of Co/PEG nanocomposite

The composition and morphology of the obtained nanometallic polymer composites of Co/PEG was evaluated using X-ray phase analysis and TEM.

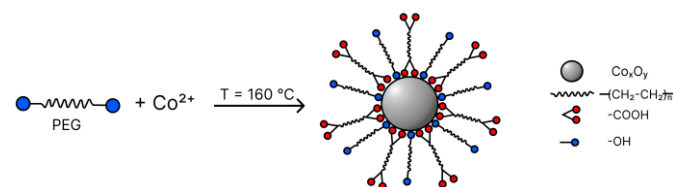
XRD data showed that all samples contained PEG matrix reflections at  $2\theta$  angles of 19.14°, 23.35°, 26.25°, 26.97°. X-ray phase analysis showed the presence of  $\text{Co}_3\text{O}_4$  nanoparticles in the Co/PEG-1 sample at  $2\theta$  angles of 30.96°, 55.64°.



**Figure 3** Profiles of intensity of characteristic bands in the FT-IR diffuse reflectance spectra of the  $\text{CoCl}_2$ -PEG mixture depending on the heating ( $T = 35\text{--}230$  °C,  $\nu_{\text{Co(II)}}/\nu_{\text{OH(PEG)}} = 1:10$ ).



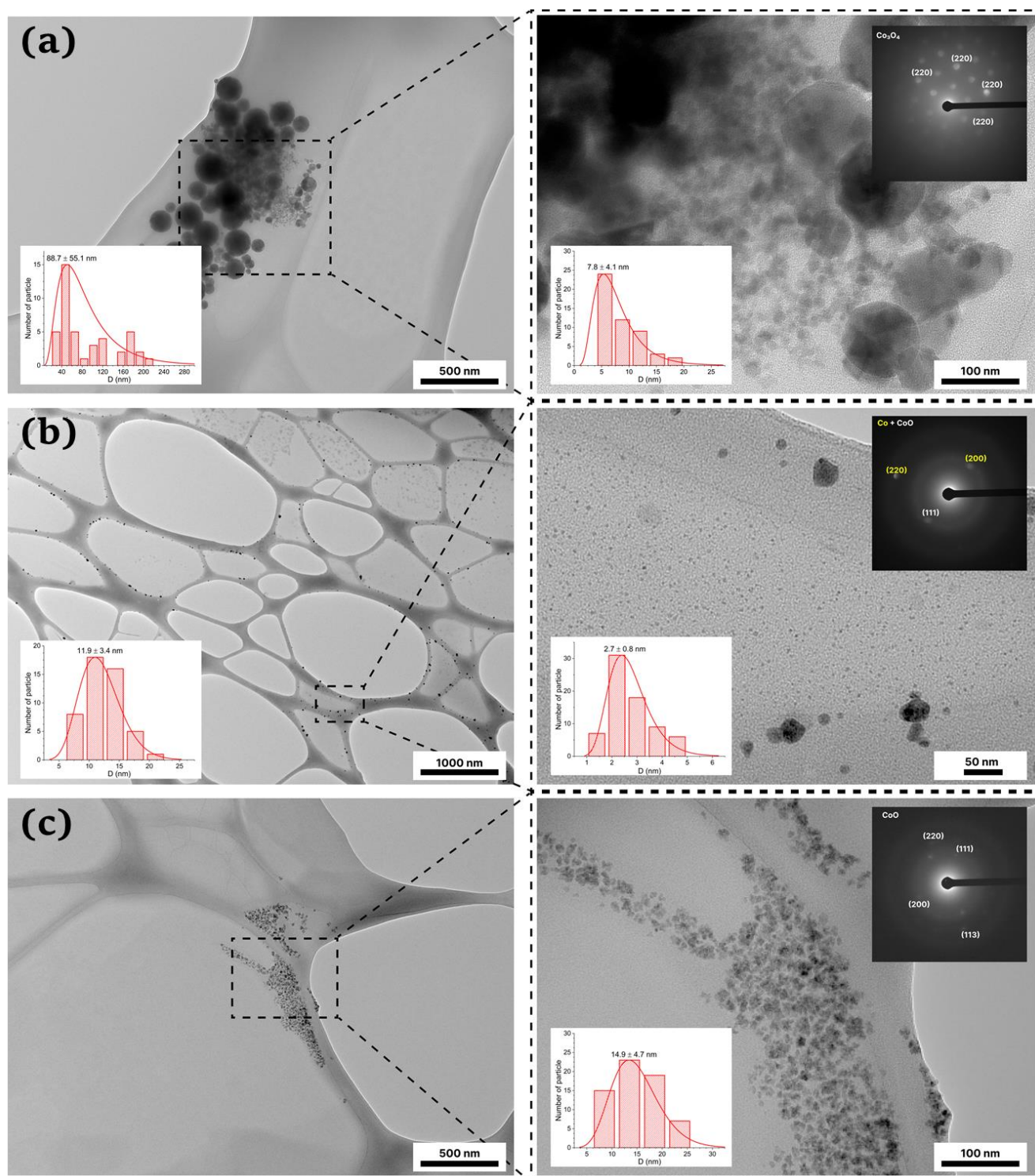
**Figure 4** FT-IR spectra of PEG and obtained nanocomposites Co/PEG.



**Figure 5** Preparation of Co/PEG nanocomposite by PEG-based polyol process.

For the Co/PEG-2 sample, the presence of  $\alpha$ -Co, the corresponding signals were observed at  $2\theta$  angles equal to 45.06°, 47.46°, and the oxide phase CoO, the signals of which were observed at  $2\theta$  angles equal to 32.68°, 43.03° and 50.00°. The synthesized Co/PEG-3 contains an oxide phase, CoO, whose signals are observed at  $2\theta$  angles of 32.68°, 43.03°, and 50.00°.

Transmission electron microscopy (TEM) and electron diffraction techniques were used to determine the morphology of the synthesized Co/PEG nanometallic polymer composites (Figure 6). For the Co/PEG-1 sample the formation of two types of polymer-stabilized nanoparticles of spheroidal shape was recorded (Figure 6a). The average diameters of the particles were  $88 \pm 55$  nm and  $8 \pm 4$  nm. The calculated parameters of the interplanar distance ( $d$ ) indicate the presence of  $\text{Co}_3\text{O}_4$ .



**Figure 6** TEM images, particle size distribution and electron diffraction of Co/PEG-1 (a), Co/PEG-2 (b) and Co/PEG-3 (c).

The Co/PEG-2 sample is characterized by the formation of two types of particles as well (Figure 6b). There are spheroidal and cluster composite nanoparticles with average diameters of  $12 \pm 3$  nm and  $3 \pm 1$  nm respectively. The calculated parameters of the interplanar distance ( $d$ ) indicate the presence of the metal phase  $\text{Co}^0$  and  $\text{CoO}$ .

The formation of scale-like structures of nanoparticles with a diameter of  $15 \pm 5$  nm was detected for the Co/PEG-3 sample (Figure 6c). The calculated parameters of the interplanar distance ( $d$ ) indicate the presence of the  $\text{CoO}$  metal phase.

### 3.5. Thermostability of Co/PEG nanocomposite

According to TG-DTG analysis the PEG polyol and the synthesized Co/PEG samples are stable in the temperature range of  $25$ – $260$  °C. Above this temperature, the polymer matrix undergoes thermal-oxidative destruction. The presence of cobalt in the composition of a metal-polymer nanocomposite leads to the increase in the thermolysis temperature by  $5$  °C. From the TG curves, the load of metallic cobalt in the samples was determined:  $0.23$ ,  $1.23$  and  $2.65\%$  for Co/PEG-1, Co/PEG-2 and Co/PEG-3 respectively.



### 3.6. Biocompatibility of Co/PEG nanocomposite

The biocompatibility of the synthesized cobalt-loaded PEG-based nanocomposites was assessed by the hemolysis coefficient (HC%) *in vitro* [32]. Substances with hemolytic activity of less than 10% are not potentially dangerous to the body and can be used for further developments in the field of biomedicine and pharmacology. The hemolytic activity of CoCl<sub>2</sub> salt, PEG (Figure 7a) and Co/PEG nanocomposites (Figure 7b) was assessed in the concentration range of 1–1000 µg·ml<sup>-1</sup>.

It was established that HC ≤ 10% at a concentration of CoCl<sub>2</sub> salt no more than C<sub>CoCl<sub>2</sub></sub> ≥ 50 µg·ml<sup>-1</sup> and for the studied polyethylene glycol at a concentration no higher than C<sub>PEG</sub> ≥ 200 µg·ml<sup>-1</sup>. The hemocompatibility of Co/PEG-1 and Co/PEG-3 nanocomposites is much better than that of Co/PEG-2. The minimum effective concentration of the nanocomposites that caused hemolysis in 50% of red blood cells (HC<sub>50</sub>) was determined. The hemolytic activity of HC<sub>50</sub> decreases in the order CoCl<sub>2</sub> (HC<sub>50</sub> = 2.82 mg·ml<sup>-1</sup>) – Co/PEG-2 (HC<sub>50</sub> = 2.91 mg·ml<sup>-1</sup>) – PEG (HC<sub>50</sub> = 3.23 mg·ml<sup>-1</sup>) – Co/PEG-3 (HC<sub>50</sub> = 4.82 mg·ml<sup>-1</sup>) – Co/PEG-1 (HC<sub>50</sub> = 6.12 mg·ml<sup>-1</sup>). The presence of Co<sup>0</sup> cluster particles in Co/PEG-2 may be the reason for the decreased biocompatibility of this composite.

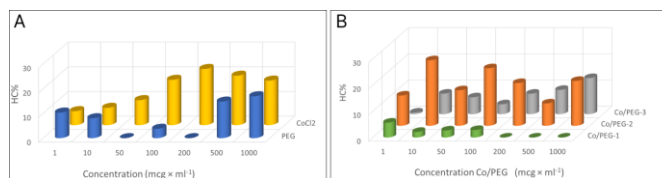
## 4. Limitations

A not obvious problem with using PEG as a stabilizer is its low melting point and amorphous nature. The nanoparticles obtained in the work must be stored at temperatures below zero to avoid their enlargement and transformation into aquatic complexes. Also, the magnetic properties must be enhanced. Therefore, in the future it is planned to study hybrid polyol stabilizers PEG / branched polyol and additionally dope them with magnetically susceptible metals such as iron and gadolinium.

## 5. Conclusions

New cobalt loaded Co/PEG nanocomposites have been synthesized. The effect of molar ration M<sup>n+</sup>/OH<sub>PEG</sub> on the formation of cobalt loaded metal-polymer nanocomposites during a one-pot two-component polyol process by a polyethylene glycol with M<sub>r</sub> = 4000 g·mol<sup>-1</sup> (PEG) was studied. Polyethylene glycol successfully acts as a reducing/stabilizing agent and a medium in the synthesis at ratios V<sub>Co2+</sub>/V<sub>OH(PEG)</sub> = 1:10, 1:100 and 1:500. The stage of preorganization of Co<sup>2+</sup> ions to the PEG matrix at a molar ratio V<sub>Co2+</sub>/V<sub>OH(PEG)</sub> of at least 1:9 is necessary.

The [Co<sup>2+</sup>-PEG]<sub>n</sub> associates with localized coordination units CoO<sub>n</sub> with tetrahedral geometry formed at this stage. The reduction of Co<sup>2+</sup> ions immobilized in PEG aggregates can be achieved by heating the reaction mixture to 160 °C in the next step to form Co/PEG nanocomposites. Part of the PEG molecules is oxidized to form carboxyl derivatives during the polyol process.



**Figure 7** Dependence of the hemolysis coefficient (HC%) on concentration CoCl<sub>2</sub>, PEG (A) and Co/PEG (B) nanocomposites (C<sub>CoCl<sub>2</sub></sub> = C<sub>PEG</sub> = C<sub>Co/PEG</sub> = 1–1000 µg·ml<sup>-1</sup>).

Oxidized and non-oxidized PEG molecules are involved in the immobilization of the cobalt nanophase. Stabilization of the cobalt nanophase occurred after 5 days, and the final stabilization of the particles of Co/PEG occurred after 14 days.

Varying the molar ration of M<sup>n+</sup>/OH<sub>PEG</sub> in a PEG-based polyol process is a promising approach to controlling the morphology of nanometallic polymer composites of M/PEG. The polyol process under conditions of V<sub>Co2+</sub>/V<sub>OH(PEG)</sub> = 1:10 leads to the formation of monomodal CoO-loaded 2D nanostructures with an average diameter D = 15±5 nm. Increasing the concentration of Co<sup>2+</sup> ions in the synthesis makes it possible to obtain bimodal Co<sup>0</sup>/CoO (V<sub>Co2+</sub>/V<sub>OH(PEG)</sub> = 1:100) and Co<sub>3</sub>O<sub>4</sub> (V<sub>Co2+</sub>/V<sub>OH(PEG)</sub> = 1:500) loaded nanostructures with an increase in the average diameter from D = 12±3 nm / 3±1 nm to D = 88±55 nm / 8±4 nm, respectively.

Controlling the size and structure of Co/PEG composite particles allows maintaining their biocompatibility. The composites Co/PEG containing only cobalt oxides (CoO or Co<sub>3</sub>O<sub>4</sub>) and having dimensions above 5 nm are hemocompatible. The hemolytic activity of HC<sub>50</sub> can reach 6.12 g·ml<sup>-1</sup>. In addition, spheroid nanocomposites have better biocompatibility compared to spherical ones and are more promising for the biomedical applications.

## • Supplementary materials

This manuscript contains supplementary materials, which are available on the corresponding online page.

## • Funding

The study was supported by a grant from the Russian Science Foundation No. 22-73-10036. (<https://rscf.ru/project/22-73-10036/>).



## • Acknowledgments

This study was supported by the Kazan Federal University Strategic Academic Leadership Program («PRIORITY-2030»). Microscopy studies were carried out at the Interdisciplinary Centre of Analytical Microscopy of Kazan Federal University.



## ● Author contributions

Conceptualization: A.B., A.K.

Data curation: A.B.

Formal Analysis: N.U.

Funding acquisition: A.K.

Investigation: L.Z., D.E., O.M., I.S.

Methodology: A.B., A.K., M.K.

Project administration: M.K.

Resources: M.K., A.K.

Supervision: M.K.

Visualization: A.B.

Writing – original draft: A.B.

Writing – review & editing: A.B., M.K.

## ● Conflict of interest

The authors declare no conflict of interest.

## ● Additional information

Author IDs:

Anastasia Burmatova, Scopus ID [58000610800](#);

Artur Khannanov, Scopus ID [56037295000](#);

Liana Zubaidullina, Scopus ID [57207882428](#);

Dmitry Emelianov, Scopus ID [57199999835](#);

Olga Mostovaya, Scopus ID [6506986848](#);

Ivan Stoikov, Scopus ID [6602887534](#);

Nikolay Ulakhovich, Scopus ID [6603803083](#);

Marianna Kutyreva, Scopus ID [6602272312](#).

Website:

Kazan Federal University, <https://eng.kpfu.ru/>.

## References

- Kharisov BI, Dias HVR, Kharissova OV. Mini-review: Ferrite nanoparticles in the catalysis. Arab J Chem. 2019;12(7):1234–1246. doi:[10.1016/j.arabjc.2014.10.049](#)
- Matsui I. Nanoparticles for electronic device applications: a brief review. J Chem Eng Japan. 2005;38(8):535–546. doi:[10.1252/jcej.38.535](#)
- Mauricio MD, Guerra-Ojeda S, Marchio P, et al. Nanoparticles in Medicine: a focus on vascular oxidative stress. Oxidative Med Cellular Longevity. 2018;2018:1–20. doi:[10.1155/2018/6231482](#)
- Zhang L, Gu F, Chan J, Wang A, Langer R, Farokhzad O. Nanoparticles in medicine: therapeutic applications and developments. Clin Pharmacol Ther. 2008;83(5):761–769. doi:[10.1038/sj.clpt.6100400](#)
- Rezić I. Nanoparticles for Biomedical application and their synthesis. Polymers. 2022;14(22):4961. doi:[10.3390/polym14224961](#)
- Ammar S, Fiévet F. Polyol synthesis: a versatile wet-chemistry route for the design and production of functional inorganic nanoparticles. Nanomater. 2020;10(6):1217. doi:[10.3390/nano10061217](#)
- Ruz P, Sudarsan V. Polyol Method for synthesis of nanomaterials. In: Tyagi AK, Ningthoujam RS, eds. Handbook on Synthesis Strategies for Advanced Materials. Indian Institute of Metals Series. Springer Singapore; 2021:293–332. doi:[10.1007/978-981-16-1807-9\\_11](#)
- Dong H, Chen YC, Feldmann C. Polyol synthesis of nanoparticles: status and options regarding metals, oxides, chalcogenides, and non-metal elements. Green Chem. 2015;17(8):4107–4132. doi:[10.1039/C5GC00943J](#)
- Li CC, Zeng HC. Cobalt (hcp) nanofibers with pine-tree-leaf hierarchical superstructures. J Mater Chem. 2010;20(41):9187. doi:[10.1039/COJM01621G](#)
- Park BK, Jeong S, Kim D, Moon J, Lim S, Kim JS. Synthesis and size control of monodisperse copper nanoparticles by polyol method. J Colloid Interface Sci. 2007;311(2):417–424. doi:[10.1016/j.jcis.2007.03.039](#)
- Soumare Y, Garcia C, Maurer T, et al. Kinetically controlled synthesis of hexagonally close-packed cobalt nanorods with high magnetic coercivity. Adv Funct Mater. 2009;19(12):1971–1977. doi:[10.1002/adfm.200800822](#)
- Gautam A, Singh GP, Ram S. A simple polyol synthesis of silver metal nanopowder of uniform particles. Synthetic Metals. 2007;157(1):5–10. doi:[10.1016/j.synthmet.2006.11.009](#)
- Burmatova A, Khannanov A, Gerasimov A, et al. A hyperbranched polyol process for designing and manufacturing nontoxic cobalt nanocomposite. Polymers. 2023;15(15):3248. doi:[10.3390/polym15153248](#)
- Navaladian S, Viswanathan B, Viswanath RP, Varadarajan TK. Thermal decomposition as route for silver nanoparticles. Nanoscale Res Lett. 2007;2(1):44. doi:[10.1007/s11671-006-9028-2](#)
- Izu N, Matsubara I, Uchida T, Itoh T, Shin W. Synthesis of spherical cobalt oxide nanoparticles by a polyol method. J Ceram Soc Japan. 2017;125(9):701–704. doi:[10.2109/jcersj2.17114](#)
- Logutenko OA, Titkov AI, Vorob'yov AM, et al. Effect of molecular weight of sodium polyacrylates on the size and morphology of nickel nanoparticles synthesized by the modified polyol method and their magnetic properties. Eur Polymer J. 2018;99:102–110. doi:[10.1016/j.eurpolymj.2017.12.017](#)
- Zhang X, Yin H, Cheng X, Jiang Z, Zhao X, Wang A. Modifying effects of polyethylene glycols and sodium dodecyl sulfate on synthesis of Ni nanocrystals in 1,2-propanediol. Appl Surface Sci. 2006;252(23):8067–8072. doi:[10.1016/j.apsusc.2005.10.010](#)
- Stiufiuc R, Iacovita C, Nicoara R, et al. One-Step synthesis of pegylated gold nanoparticles with tunable surface charge. J Nanomater. 2013;2013:1–7. doi:[10.1155/2013/146031](#)
- Stiufiuc R, Iacovita C, Lucaciuc CM, et al. SERS-active silver colloids prepared by reduction of silver nitrate with short-chain polyethylene glycol. Nanoscale Res Lett. 2013;8(1):47. doi:[10.1186/1556-276X-8-47](#)
- Díaz-Cruz C, Alonso Nuñez G, Espinoza-Gómez H, Flores-López LZ. Effect of molecular weight of PEG or PVA as reducing-stabilizing agent in the green synthesis of silver-nanoparticles. Eur Polymer J. 2016;83:265–277. doi:[10.1016/j.eurpolymj.2016.08.025](#)
- Iacovita C, Stiufiuc R, Radu T, et al. Polyethylene glycol-mediated synthesis of cubic iron oxide nanoparticles with high heating power. Nanoscale Res Lett. 2015;10(1):391. doi:[10.1186/s11671-015-1091-0](#)
- Haddad PS, Santos MC, De Guzzi Cassago CA, Bernardes JS, De Jesus MB, Seabra AB. Synthesis, characterization, and cytotoxicity of glutathione-PEG-iron oxide magnetic nanoparticles. J Nanopart Res. 2016;18(12):369. doi:[10.1007/s11051-016-3680-y](#)
- Abbas M, Nazrul Islam Md, Parvatheeswara Rao B, Ogawa T, Takahashi M, Kim C. One-pot synthesis of high magnetization air-stable FeCo nanoparticles by modified polyol method. Mater Lett. 2013;91:326–329. doi:[10.1016/j.matlet.2012.10.019](#)
- Banerjee SS, Aher N, Patil R, Khandare J. Poly(ethylene glycol)-prodrug conjugates: concept, design, and applications. J Drug Deliv. 2012;2012:1–17. doi:[10.1155/2012/103973](#)
- Lyseng-Williamson KA. Macrogol (polyethylene glycol) 4000 without electrolytes in the symptomatic treatment of chronic constipation: a profile of its use. Drugs Ther Perspect. 2018;34(7):300–310. doi:[10.1007/s40267-018-0532-0](#)

26. Aoun N, Schlange A, Dos Santos AR, Kunz U, Turek T. Effect of the OH-/Pt ratio during polyol synthesis on metal loading and particle size in DMFC catalysts. *Electrocatal*. 2016;7(1):13-21. doi:[10.1007/s12678-015-0275-9](https://doi.org/10.1007/s12678-015-0275-9)
27. Khannanov A, Burmatova A, Ignatyeva K, et al. Effect of the synthetic approach on the formation and magnetic properties of iron-based nanophase in branched polyester polyol matrix. *IJMS*. 2022;23(23):14764. doi:[10.3390/ijms232314764](https://doi.org/10.3390/ijms232314764)
28. Khannanov A, Rossova A, Ulakhovich N, et al. Doxorubicin-loaded hybrid micelles based on carboxyl-terminated hyperbranched polyester polyol. *ACS Appl Polym Mater*. 2022;4(4):2553-2561. doi:[10.1021/acsapm.1c01863](https://doi.org/10.1021/acsapm.1c01863)
29. Malloy A, Hole P, Carr B. Nanoparticle tracking analysis; the halo system. *MRS Proc*. 2006;952:0952-F02-04. doi:[10.1557/PROC-0952-F02-04](https://doi.org/10.1557/PROC-0952-F02-04)
30. Kashkanova AD, Blessing M, Gemeinhardt A, Soulat D, Sandoghdar V. Precision size and refractive index analysis of weakly scattering nanoparticles in polydispersions. *Nat Methods*. 2022;19(5):586-593. doi:[10.1038/s41592-022-01460-z](https://doi.org/10.1038/s41592-022-01460-z)
31. Dragovic RA, Gardiner C, Brooks AS, et al. Sizing and phenotyping of cellular vesicles using nanoparticle tracking analysis. *Nanomed Nanotechnol Biol Med*. 2011;7(6):780-788. doi:[10.1016/j.nano.2011.04.003](https://doi.org/10.1016/j.nano.2011.04.003)
32. Klajnert B, Walach W, Bryszewska M, Dworak A, Shcharbin D. Cytotoxicity, haematotoxicity and genotoxicity of high molecular mass arborescent polyoxyethylene polymers with polyglycidol-block-containing shells. *Cell Biol Int*. 2006;30(3):248-252. doi:[10.1016/j.cellbi.2005.10.026](https://doi.org/10.1016/j.cellbi.2005.10.026)
33. Parveen S, Sahoo SK. Nanomedicine: clinical applications of polyethylene glycol conjugated proteins and drugs. *Clin Pharmacokinet*. 2006;45(10):965-988. doi:[10.2165/00003088-200645100-00002](https://doi.org/10.2165/00003088-200645100-00002)
34. Ren J, Lin T, Sprague LW, Peng I, Wang LQ. Exploring chemical equilibrium for alcohol-based cobalt complexation through visualization of color change and UV-vis spectroscopy. *J Chem Educ*. 2020;97(2):509-516. doi:[10.1021/acs.jchemed.9b00264](https://doi.org/10.1021/acs.jchemed.9b00264)
35. Aranishi K, Zhu Q, Xu Q. Dendrimer-encapsulated cobalt nanoparticles as high-performance catalysts for the hydrolysis of ammonia borane. *ChemCatChem*. 2014;6(5):1375-1379. doi:[10.1002/cctc.201301006](https://doi.org/10.1002/cctc.201301006)
36. Imadadulla M, Nemakal M, Koodlur Sannegowda L. Solvent dependent dispersion behaviour of macrocycle stabilized cobalt nanoparticles and their applications. *New J Chem*. 2018;42(14):11364-11372. doi:[10.1039/C8NJ01773E](https://doi.org/10.1039/C8NJ01773E)
37. Alrehaily LM, Joseph JM, Biesinger MC, Guzonas DA, Wren JC. Gamma-radiolysis-assisted cobalt oxide nanoparticle formation. *Phys Chem Chem Phys*. 2013;15(3):1014-1024. doi:[10.1039/C2CP43094K](https://doi.org/10.1039/C2CP43094K)
38. Singh J, Tripathi J, Kaurav N. Synthesis and characterization of Co nanoparticles. *AIP Conf Proc*. 2017;050083. doi:[10.1063/1.4980316](https://doi.org/10.1063/1.4980316)
39. Spiridonov VV, Sybachin AV, Pigareva VA, et al. One-step low temperature synthesis of CeO<sub>2</sub> nanoparticles stabilized by carboxymethylcellulose. *Polymers*. 2023;15(6):1437. doi:[10.3390/polym15061437](https://doi.org/10.3390/polym15061437)